

Supporting information

Co doping modulates the electronic structure of nickel
diselenide and promotes the simultaneous occurrence of
glycerol oxidation and hydrogen evolution reactions

Hanbin Jin^a, Xiaoling Zhou^a, Lulu Guo^a, Qingtao Wang^{a,*}, Yanxia Wu^{a,*}

a Key Laboratory of Eco-functional Polymer Materials of the Ministry of Education,
Key Laboratory of Eco-environmental Polymer Materials of Gansu Province, College
of Chemistry and Chemical Engineering, College of Engineering, Northwest Normal
University, Lanzhou 730070, China

Yanxia Wu: wuyx2014@nwnu.edu.cn

Qingtao Wang: wangqt@nwnu.edu.cn

Experimental Section

Raw materials

Selenium powder is purchased from McLean, nickel nitrate is produced by Shanghai Zhongqin Chemical Reagent Co., Ltd., cobalt nitrate is supplied by Adamas Beta (Shanghai) Chemical Reagent Co., Ltd., potassium hydroxide is provided by Shanghai Wokai Biotechnology Co., Ltd., sodium hydroxide and isopropanol are obtained from China National Pharmaceutical Group Chemical Reagent Co., Ltd., glycerin is sourced from Aladdin Reagents (Shanghai) Co., Ltd., and Nafion solution is produced by Alfa Aesar Chemical Co.

Synthesis of Co-NiSe₂

Weigh nickel nitrate (1-x mmol) and cobalt nitrate (x mmol) in the ratios of $x = 0, 0.05, 0.1, 0.15, 0.2$ mmol, ensuring the total molar amount is 1 mmol. Dissolve the metal salts in 25 mL of deionized water to prepare Solution 1. Weigh 4 g of NaOH and 2 mmol of selenium powder, and dissolve them in 5 mL of deionized water to create Solution 2. Combine Solutions 1 and 2, and stir the mixture for 30 min. Transfer the resulting solution to a 50 mL reaction vessel and conduct a hydrothermal reaction at 200 °C for 10 h. After cooling, wash the product with deionized water and anhydrous ethanol, then filter it. Dry the product under vacuum at 50 °C overnight to obtain cobalt-doped nickel selenide catalysts with varying compositions^[1, 2].

Material characterization

The phase and structural testing of the experimental samples was conducted using a D8 ADVANCE X-ray diffractometer from Bruker, Germany. The testing conditions were as follows: scanning speed of 10°/min; scanning range from 10° to 80°; and X-ray source of Cu K α ($\lambda = 1.5418$ Å). For morphological analysis of the prepared

samples, an ULTRA plus field emission scanning electron microscope (FE SEM) from Carl Zeiss, USA, was utilized. The microstructure of the prepared materials was examined using a TF20 transmission electron microscope from FEI, USA. The specific testing process involved taking a small amount of the sample and placing it in a centrifuge tube, adding an appropriate volume of ethanol solvent, and ultrasonically dispersing it for 10 min. Once the sample was evenly dispersed, a suitable amount was pipetted and deposited onto a microgrid, which was then dried prior to testing and observation^[3]. Using the ESCALABXI⁺X-ray photoelectron spectrometer (XPS) from Thermo Fisher Scientific, we analyzed the valence states and composition of the surface elements of the samples. The XPS spectra were calibrated using the C 1s peak at 284.8 eV^[4].

Preparation of catalyst electrodes

Weigh 5 mg of catalyst into a sample tube. Add 20 μL of Nafion and 980 μL of DMF solution, then sonicate for 1 h to create a homogeneous solution. Next, use a pipette to transfer 25 μL of the solution and coat it onto the surface of carbon paper. Allow the coated carbon paper to air dry naturally before testing. The carbon paper is treated with 0.5 mol L^{-1} hydrochloric acid, acetone, alcohol, and deionized water, with each treatment sonicated for 15 min and then dried at 60 $^{\circ}\text{C}$ before use. The dimensions of the carbon paper are $1 \times 1 \text{ cm}^2$, resulting in a catalyst loading of 0.2 mg cm^{-2} .

Electrochemical performance testing

All electrochemical measurements were conducted on the Autolab PGSTA T128N electrochemical workstation using a three-electrode system,. The 10% Co-NiSe₂ sample served as the working electrode, with Hg/HgO functioning as the reference electrode and a platinum sheet as the counter electrode. The experimental potential was converted to the RHE using the equation $E = E(\text{Hg}/\text{HgO}) + 0.059 \text{ pH} + 0.098$ ^[5]. The electrocatalytic HER performance of the catalyst in 1 mol L^{-1} KOH electrolyte was tested using LSV or CV^[6]. Electrochemical impedance spectroscopy measurements are

performed over a frequency range of 50 kHz to 0.01 Hz, under the open-circuit voltage corresponding to the electrodes. The charge transfer resistance (R_{ct}) is calculated from the diameter of the semicircle in the Nyquist plot. The double-layer capacitance (C_{dl}) is determined through CV at various scan rates. $ECSA = 1 * C_{dl} / C_s$, in which the 1 is geometric area of the electrode, C_s represents the average specific capacitance of flat surfaces and its value in alkaline media is 0.040 mF cm^{-2} [7] The stability of the catalyst is assessed by analyzing the polarization curves before and after continuous CV cycling, as well as monitoring the change in test potential over time at a constant current density[8]. All of the above electrochemical tests were conducted without iR compensation.

Product Testing and Analysis

To determine the oxidation products of glycerol and calculate the corresponding Faradaic efficiency, experiments were conducted in an H-type electrolysis cell, utilizing 10% Co-NiSe₂ self-supporting electrodes as both the anode and cathode working electrodes. The cathode underwent a steady-state constant current test at a current density of 100 mA cm^{-2} , and hydrogen gas production was collected using a drainage method to calculate the Faradaic efficiency of hydrogen. Similarly, the anode was operated at a fixed current density of 100 mA cm^{-2} . After 2 h, a specific volume of the electrolyte solution was collected and analyzed using a nuclear magnetic resonance (NMR) spectrometer. In preparation for NMR analysis, 200 μL of the electrolyte solution, and 6 mL of DMSO were sequentially added to the NMR tube and sonicated for 10 min. The Faradaic efficiency (%) for the production of H₂ and formate was estimated using the following equations: $FE (\%) = 100\% \times V (\text{H}_2 \text{ production}) / (QV_s/\alpha F)$ and $FE (\%) = 100\% \times n (\text{formate production}) / (Q/\alpha F)$, where Q represents the total charge consumed during electrolysis, V_s is the standard molar volume (22.4 L mol^{-1}), F is Faraday's constant ($96,485 \text{ C mol}^{-1}$), and α is the number of electrons required to produce H₂ molecules ($\alpha = 2$) and for formate ($\alpha = 8/3$)[9-13]. The formula for calculating the stability decay rate is: $\text{Decay Rate} = [(\text{Initial Voltage} - \text{Final Voltage})$

/ Initial Voltage] * 100%.

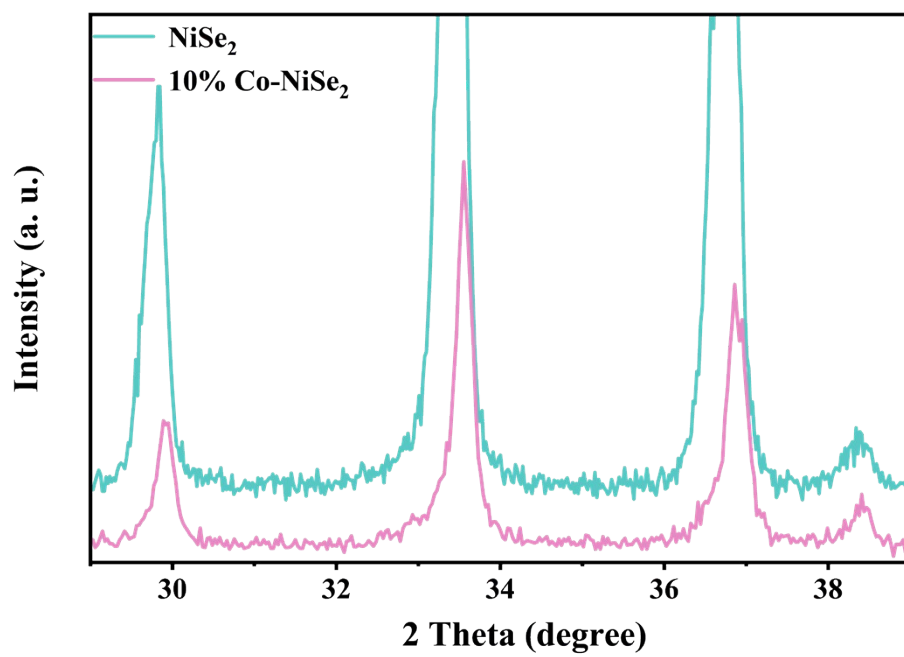


Figure S1 Local magnification of XRD.

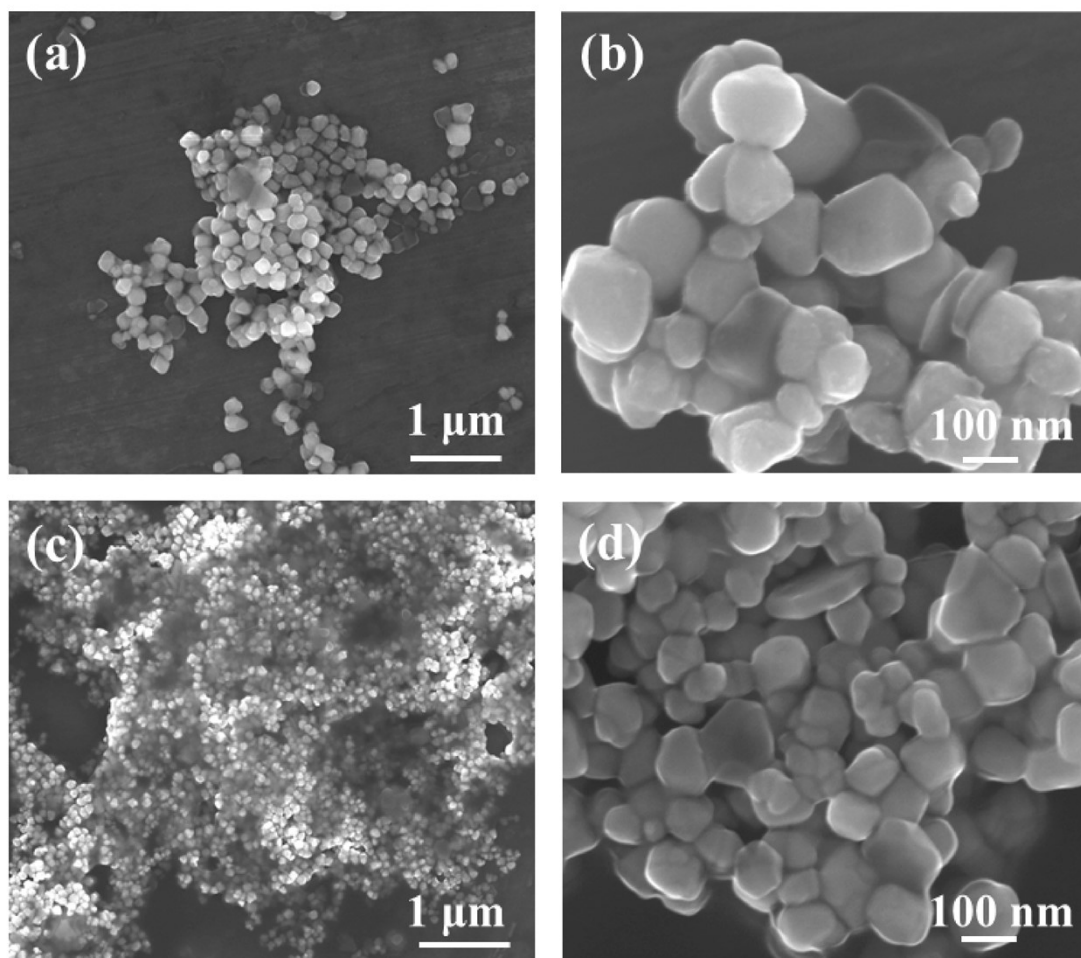


Figure S2 (a, b) SEM images of NiSe₂ at different resolutions. (c, d) SEM images of 10% Co-NiSe₂ at different resolutions.

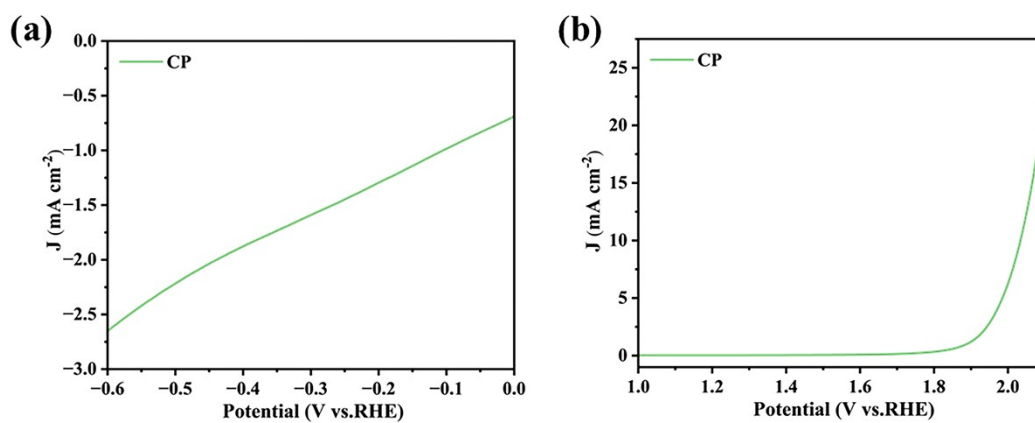


Figure S3 Electrochemical Performance Testing of Carbon Paper. (a) HER; (b)GOR.

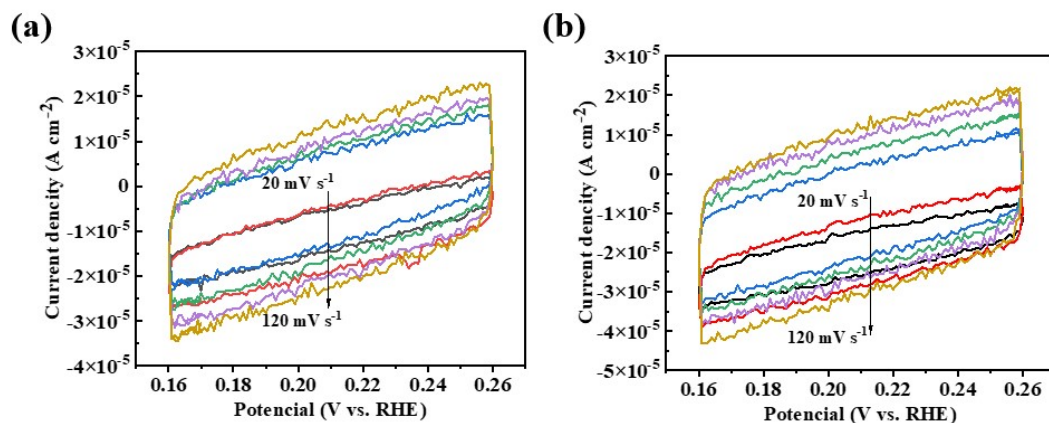


Figure S3 CV curves at different scan rates in the non-faraday range during the hydrogen evolution reaction: (a) NiSe_2 and (b) 10% Co-NiSe_2 .

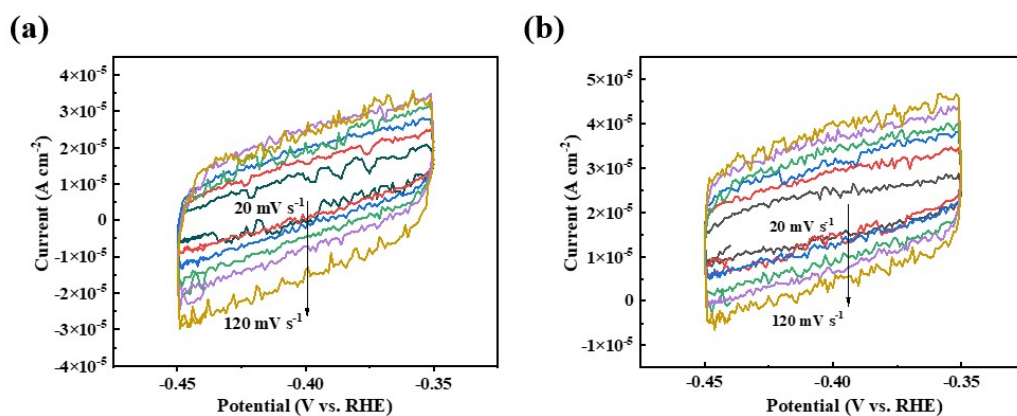


Figure S4 CV curves at different scan rates in the non-faraday range during the GOR: (a) NiSe_2 and (b) 10% Co-NiSe_2 .

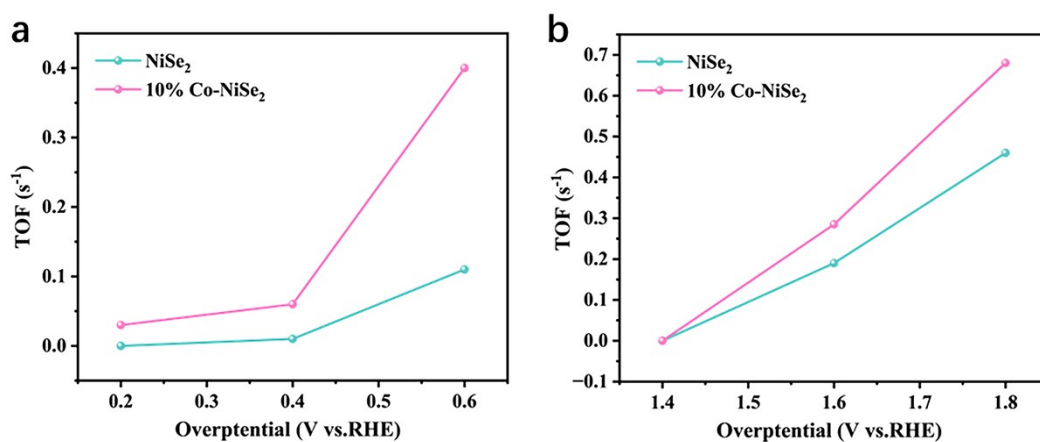


Figure S5 (a) TOF calculation of 10% Co-NiSe_2 and NiSe_2 in HER, (b) TOF calculation of 10% Co-NiSe_2 and NiSe_2 in GOR.

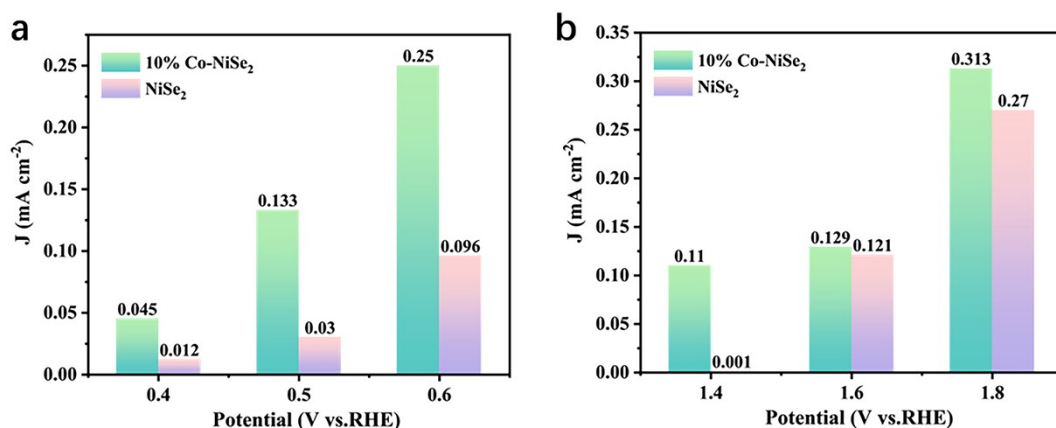


Figure S6 The electrochemical surface area normalized current densities of 10% Co-NiSe₂ and NiSe₂.(a) HER,(b) GOR.

Table S1: Comparison of the performance of 10%Co-NiSe₂ with other catalysts.

Catalyst	Electrolyte	Value-added products	J (mA cm^{-2})	Voltage (V)	Ref
10%Co-NiSe ₂	1 M KOH +0.1 M Gly	fromate	10	1.45	This work
NC@CuCo ₂ N _x /CF	1 M KOH +0.15 M BA	benzyl alcohol	10	1.62	[14]
Ni-Mo-N/CFC	1.0 M KOH +0.1 M Gly	fromate	10	1.36	[15]
LMOS-4	1 M KOH	O ₂	10	1.58	[16]
Eu ₃ O ₄ /WO _x	1.0 M KOH +0.1 M Gly	fromate	10	1.52	[17]
Co-Rh ₂	1 M KOH +1 M CH ₃ OH	HCOH	10	1.54	[18]

Reference

- [1] LIANG J, YANG Y, ZHANG J, et al. Metal diselenide nanoparticles as highly active and stable electrocatalysts for the hydrogen evolution reaction [J]. *Nanoscale*, 2015, 7(36): 14813-6.
- [2] XU K, DING H, LV H, et al. Understanding Structure-Dependent Catalytic Performance of Nickel Selenides for Electrochemical Water Oxidation [J]. *ACS Catalysis*, 2016, 7(1): 310-5.
- [3] SUN Y, XU K, WEI Z, et al. Strong Electronic Interaction in Dual-Cation-Incorporated NiSe(2) Nanosheets with Lattice Distortion for Highly Efficient Overall Water Splitting [J]. *Adv Mater*, 2018, 30(35): e1802121.
- [4] DAI J, ZHAO D, SUN W, et al. Cu(II) Ions Induced Structural Transformation of Cobalt Selenides for Remarkable Enhancement in Oxygen/Hydrogen Electrocatalysis [J]. *ACS Catalysis*, 2019, 9(12): 10761-72.
- [5] LIU X, ALBLOUSHI M, GALVIN M, et al. A paired alkaline electrolyzer for furfural oxidation and hydrogen evolution over noble metal-free NiFe/Ni and Co/MXene catalysts [J]. *Green Chemistry*, 2024, 26(22): 11351-63.
- [6] WANG G, CHEN J, CAI P, et al. A self-supported Ni-Co perselenide nanorod array as a high-activity bifunctional electrode for a hydrogen-producing hydrazine fuel cell [J]. *Journal of Materials Chemistry A*, 2018, 6(36): 17763-70.
- [7] MCCRORY C C L, JUNG S, PETERS J C, et al. Benchmarking Heterogeneous Electrocatalysts for the Oxygen Evolution Reaction [J]. *Journal of the American Chemical Society*, 2013, 135(45): 16977-87.
- [8] XIE X, ZHANG C, XIANG M, et al. SnO₂/CoS_{1.097} heterojunction as a green electrocatalyst for hydrogen evolution linking to assistant glycerol oxidation [J]. *Green Chemistry*, 2023, 25(22): 9405-12.
- [9] LIMA C C, RODRIGUES M V F, NETO A F M, et al. Highly active Ag/C nanoparticles containing ultra-low quantities of sub-surface Pt for the electrooxidation of glycerol in alkaline media [J]. *Applied Catalysis B: Environmental*, 2020, 279.
- [10] PEI Y, PI Z, ZHONG H, et al. Glycerol oxidation-assisted electrochemical CO₂ reduction for the dual production of formate [J]. *Journal of Materials Chemistry A*, 2022, 10(3): 1309-19.
- [11] HAMEED A, BATOOL M, LIU Z, et al. Layered Double Hydroxide-Derived Nanomaterials for Efficient Electrocatalytic Water Splitting: Recent Progress and Future Perspective [J]. *ACS Energy Letters*, 2022, 7(10): 3311-28.
- [12] DU H, WANG K, TSIKARAS P, et al. Excavated and dendritic Pt-Co nanocubes as efficient ethylene glycol and glycerol oxidation electrocatalysts [J]. *Applied Catalysis B: Environmental*, 2019, 258.
- [13] SHI K, SI D, TENG X, et al. Enhanced electrocatalytic glycerol oxidation on CuCoN_{0.6}/CP at significantly reduced potentials [J]. *Chinese Journal of Catalysis*, 2023, 53: 143-52.
- [14] ZHENG J, CHEN X, ZHONG X, et al. Hierarchical Porous NC@CuCo Nitride Nanosheet Networks: Highly Efficient Bifunctional Electrocatalyst for Overall Water Splitting and Selective Electrooxidation of Benzyl Alcohol [J]. *Advanced Functional Materials*, 2017, 27(46).
- [15] LI Y, WEI X, CHEN L, et al. Nickel-molybdenum nitride nanoplate electrocatalysts for concurrent electrolytic hydrogen and formate productions [J]. *Nature Communications*, 2019, 10(1).
- [16] SHIT S, BOLAR S, MURMU N C, et al. Minimal lanthanum-doping triggered enhancement in bifunctional water splitting activity of molybdenum oxide/sulfide heterostructure through structural evolution [J]. *Chemical Engineering Journal*, 2022, 428.

- [17] YANG Z, NIU H, XIA L, et al. Rare-earth europium heterojunction electrocatalyst for hydrogen evolution linking to glycerol oxidation [J]. International Journal of Hydrogen Energy, 2023, 48(83): 32304-12.
- [18] GUO Y, YANG X, LIU X, et al. Coupling Methanol Oxidation with Hydrogen Evolution on Bifunctional Co-Doped Rh Electrocatalyst for Efficient Hydrogen Generation [J]. Advanced Functional Materials, 2022, 33(2).